INTL JOURNAL OF ELECTRONICS AND TELECOMMUNICATIONS, 2023, VOL. 69, NO. 3, PP. 449-454
Manuscript received May 3, 2023; revised July, 2023. DOI: 10.24425/ijet.2023.144382

Bandwidth Enhancement for Half Mode Substrate Integrated Waveguide Antenna using Defected Ground Structures

Dian Widi Astuti*, Rivayanto, Muslim, Imelda Simanjuntak, Teguh Firmansyah, Dwi Astuti Cahyasiwi, and Yus Natali

***Abstract*—The SIW antenna suffers from the narrow bandwidth for a single cavity and single resonant. Defected ground structure (DGS) with a dual cavity was the solution to solve narrow bandwidth by resulting in hybrid resonance. The hybrid resonance with 14.83% impedance bandwidth is proposed in this antenna design. The first resonance resulted from the combination of the TE_{101} modes from inner and outer HMSIW cavities while the second resonance resulted from the combination of the strong TE_{101} and the weak TE_{102} mode from the inner HMSIW cavity and the addition of the weak TE_{101} from the outer HMSIW cavity. The measurement antenna design has a broadband antenna with a 14.31% (5.71 – 6.59 GHz) impedance bandwidth by using substrate Rogers RO 5880.**

***Keywords*—Bandwidth enhancement; dual cavity; half mode substrate integrated waveguide; defected ground structure; U-slot**

I. Introduction

TELECOMMUNICATION grows rapidly to fulfill human needs. It caused rapid research into the components of telecommunication, one of which is antennas. A low profile, small, system on a substrate (SoS) and broadband antennas are such interesting topics of research for antennas. Substrate integrated waveguide (SIW) antenna can fulfill these requirements. SIW offers a low profile with a high-quality factor antenna [1]. However, a low-profile antenna with single resonance cause limitation for frequency application in telecommunication [2]. Various kinds of methods have been proposed to enhance impedance bandwidth such as substrate removal [3], mode superimposition by using modification slots [4]–[6] and defected ground structures (DGS) [7].

Ref. [3] changes the Q-factor of the antenna by removing the substrate under the slot. The 2.16% impedance bandwidth measured can be achieved by this method and it has 24% wider than the conventional SIW antenna. However, removing some substrate under the slot is not an easy task. Another method for bandwidth enhancement is achieved by mode superimposition that results in a hybrid [4], [5], and triple resonance [6]. Hybrid resonance on the Ref [4] has improved impedance bandwidth up to 6.3% compared with a single resonance in the previous report [2]. Hybrid resonance consists of a stronger or weak combination between TE_{101} and TE_{102} modes and it is achieved by using a non-resonant slot. The rectangular slot as a non-resonant slot was modified into a bow tie slot [5], and it results in a 9.8% impedance bandwidth improvement.

In Ref. [6] triple resonance succeed enhancing impedance bandwidth up to 8.5 % by using dual-unequal-slot. The dual-unequal-slot generate two resonance frequency close to each other. The circuit equivalent for each slot is modeled by a shunt conductance and a susceptance. However, the impedance bandwidth from Ref. [3]–[6] is still below 10%.

Another method for enhancing impedance bandwidth is defected ground structure (DGS) on the ground layer as shown in Ref. [7], [8]. Early, the DGS has implemented successfully on the filter component for suppressing higher mode harmonic and mutual coupling [9], [10]. By using DGS as the U-slot, Ref. [7] has improved impedance bandwidth to 14.5%. However, the structure is still larger because of the full-mode structure.

The small antennas are related to miniaturization antennas while the SoS related to with integration of other components on the same substrate. All of these requirements can be done easily on the SIW antenna. Miniaturization can be achieved by dividing full mode into sub-cavities i.e. half mode SIW (HMSIW), quarter mode SIW (QMSIW), eight mode SIW (EMSIW) until sixth mode SIW (SMSIW). Again, the sub-cavities of SIW with a dominant mode suffer the narrow bandwidth [11]–[13]. Some research is concerned to enhance impedance bandwidth by using fraction mode [14], coupling [15], dual cavity [16], [17], or modified slot [18], [19]. All of this research has succeeded in improving impedance bandwidth by generating hybrid, triple and quad resonance. However, impedance bandwidth improvement is still below 14%.

This paper presents impedance bandwidth improvement by using defected ground structure in the form of a U-slot. The U-slot has improved impedance bandwidth by up to 14% with 50% miniaturization. Miniaturization occurs due to the use of the

This work was supported by Universitas Mercu Buana, Jakarta Indonesia on the Kerjasama Dalam Negeri (KDN) research in 2021 under contract 02-5/196/B-SPK/II/2021.

Dian Widi Astuti, Rivayanto, Muslim and Imelda Simanjuntak are with Department of Electrical Engineering, Universitas Mercu Buana, Jakarta, Indonesia (e-mail: dian.widiastuti@mercubuana.ac.id, rivayanto802@gmail.com, muslim@mercubuana.ac.id).

Teguh Firmansyah is with Department of Electrical Engineering, Universitas Sultan Ageng Tirtayasa, Serang, Indonesia (e-mail: teguhfirmansyah@untirta.ac.id).

Dwi Astuti Cahyasiwi is with Department of Electrical Engineering, Universitas Muhammadiyah Prof. Dr. HAMKA, Jakarta, Indonesia (e-mail: dwi.cahyasiwi@uhamka.ac.id).

Yus Natali is with Telecommunication Program, Universitas Telkom, Jakarta, Indonesia (e-mail: yusnatali@telkomuniversity.ac.id).

HMSIW structure. A low profile and miniaturization are achieved of the prototype antenna by using $0.03\lambda_0$ (at 5.71 GHz) substrate thickness.

II. Antenna Design

The antenna design used Rogers 5880 fabric substrate with a relative permittivity of $\varepsilon_r = 2.2$, a thickness of $h = 1.575$ mm, and a loss tangent of the substrate $\delta = 0.0009$. The rectangular SIW has a row of holes with a hole diameter, d, and the center distance between two adjacent center holes, p. For reducing the leakage of energy, $d/p \geq 0.5$ and $d/\lambda_0 \leq 0.1$ have been fulfilled where λ_0 is the free-to-air wavelength [20]. The fed line connector was placed on the ground layer. Ansys HFSS is used as an electromagnetic simulator tool for antenna design.

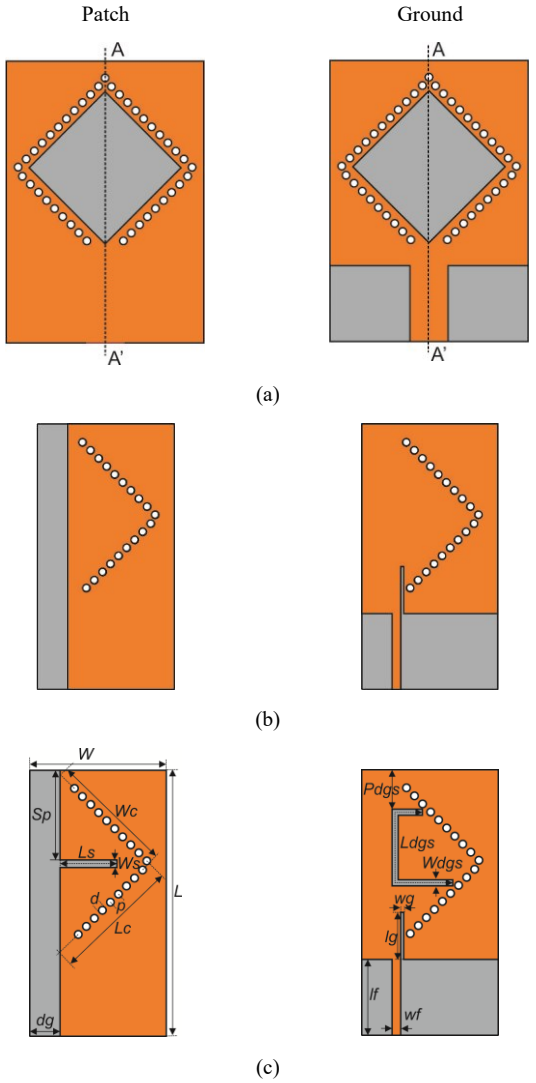

Fig. 1. Transformation antenna design: (a) Ant-A with the full mode SIW (FMSIW), (b) Ant-B with the half mode SIW (HMSIW), (c) Ant-C with DGS. ($W = 18$, $L = 35$, $Sp = 11.8$, $Wc =$, $Lc =$, $Ls = 7.5$, $Ws = 1$, $d = 1$, $p = 1.5$, $dg = 4$, $Pdgs = 5.2$, $Ldgs = 20.5$, $Wdgs = 0.8$, $wg = 0.4$, $lg = 6.2$, $wf = 1.14$, $lf = 10$. All units in mm)

A. Antenna Evolution

The antenna design is achieved by the transformation from the full mode SIW (FMSIW) into the half mode SIW (HMSIW) with defected ground structure (DGS) as shown in Fig. 1. The reflection coefficient for the transformation antenna design is shown in Fig. 2.

The resonant frequency mode for Ant-A can be counted based on [21]. Ant-A design use 6 GHz as the frequency cut-off for the outer cavity as shown in Fig. 1(a). The outer cavity consists of four QMSIWs structure and the TE_{101} mode shift into higher frequency because of its structure. The reflection coefficient Ant-A occurs on 6.60 – 6.94 GHz. It means the 5.02% impedance bandwidth was achieved which is caused by the TE_{101} mode on the four QMSIWs structure. Ant-B is achieved by adding the inner part and dividing becomes two-part symmetrically (AA'). Each part is called half mode SIW (HMSIW) as shown in Fig. 1(b). The TE_{101} modes from the inner HMSIW and the outer HMSIW (two parts of QMSIWs) are resonant contiguous as shown in Fig. 2. The TE_{101} mode from the outer HMSIW shifts into the lower frequency that resonant on 5.94 – 6.25 GHz (5.09%), while the TE_{101} mode from the inner HMSIW resonance on 8.04 – 8.26 GHz (2.70%). It can be seen that Ant-A and Ant-B suffer from the narrow bandwidth because of single resonance.

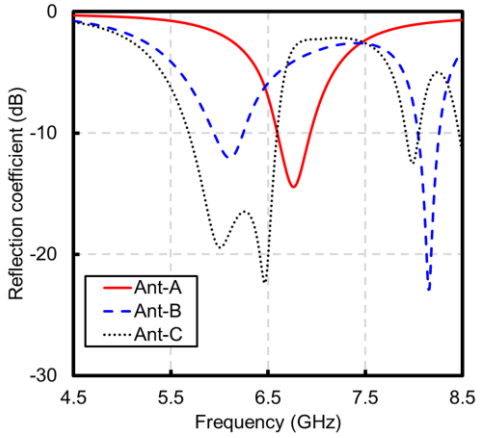

Fig. 2. Reflection coefficient for transformation antenna design

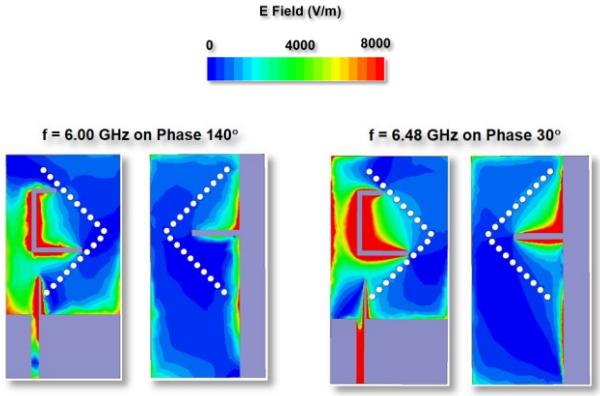

Fig. 3. The electric field distribution on (a) 6.00 GHz, (b) 6.48 GHz of antenna design (Ant-C).\

Furthermore, Ant-C has a rectangular slot on the patch and a U-slot on the ground. This aim is to enhance bandwidth by joint together the two TE_{101} modes as shown in Fig. 2. It results in 14.83% bandwidth enhancement that works on 5.68 – 6.59 GHz

with hybrid resonance. The final antenna design as shown in Ant-C works out three times of impedance bandwidth than Ant-A and Ant-B.

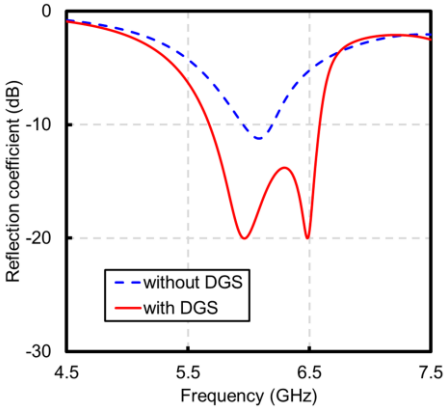

Fig. 4. The reflection coefficient for antenna design (Ant-C) without DGS and with DGS

B. Electric Field Distribution

Hybrid resonance of Ant-3 occurs at 6.00 GHz and 6.48 GHz. The radiator slot changes into the DGS. It occurs because the DGS is near the fed line. The electric field distribution of each resonant frequency is shown in Fig. 3. The electric field distribution on 6.00 GHz occurs because of the combination of the TE_{101} modes from the inner and the outer HMSIW cavities as shown in Fig. 3(a). While the second resonance resulted from the combination of the strong TE_{101} and the weak TE_{102} mode from the inner cavity and the addition of the weak TE_{101} from the outer cavity as shown in Fig. 3(b). The electric field distribution has the same scale of 8000 V/m.

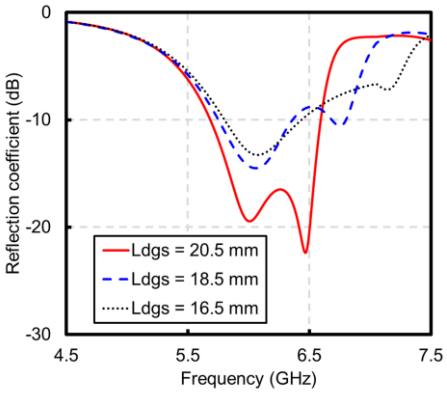

(a)

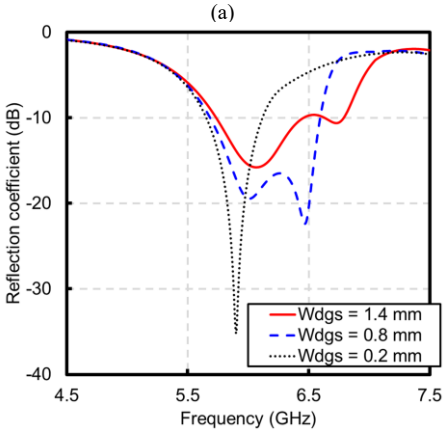

(b)

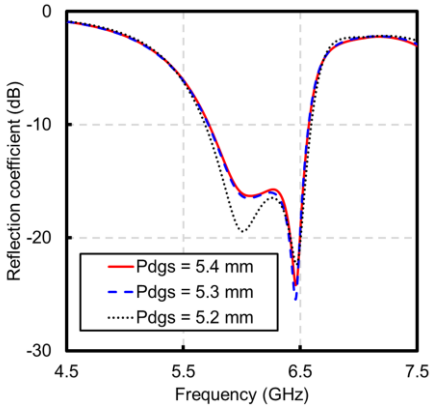

(c)

Fig. 5. Reflection coefficient plots for different: (a) the length, 'L_{dgs}', (b) the width, 'W_{dgs}' and (c) slot position 'P_{dgs}' of U-slot as a DGS structure

C. Parameters Studies

Bandwidth enhancement of the antenna design was influenced by DGS on the ground layer as shown in Fig. 4. The antenna design without DGS has a 3.45% impedance bandwidth that works on 5.98 – 6.19 GHz. While by adding a U-slot as a DGS on the ground layer, the antenna design has 14.83% (5.68 – 6.59 GHz) impedance bandwidth. The DGS has improved bandwidth enhancement up to 4.3 times rather than the antenna design without DGS.

The U-slot itself was influenced by the length, width, and position of the U-slot as shown in Fig. 5. The position U-slot is measured according to the upper edge of the substrate antenna. Fig. 5(a) shows the length of the U-slot influences the second resonant of hybrid resonance. According to the electric field distribution shown that the second resonant resulted from the weak TE_{102} and the strong TE_{101} from the inner HMSIW cavity and the addition of the weak TE_{101} from the outer HMSIW cavity. Because the U-slot was located on the inner HMSIW, the electric distribution of the TE_{101} and TE_{102} modes from the inner HMSIW is more influenced by the U-slot length. The U-slot length has succeeded in shifting the TE_{101} and TE_{102} from the inner HMSIW into the lower frequency and merges with the TE_{101} from the outer HMSIW to enhance impedance bandwidth.

The width of the U-slot also influences hybrid resonance as shown in Fig. 5(b). By the same length and position of the U-slot, the width of the U-slot has to choose for generating hybrid resonance. The width of the U-slot influences the electric field distribution that comes out of the slot gap from the inner HMSIW. If the width of the U-slot is too thin, the combination of the TE_{101} and the TE_{102} modes disappear rather than the width of the U-slot being wide enough. The thinness of the U-slot makes this antenna design has a single resonance with a narrow impedance bandwidth.

The slot position of the U-slot is not too influence bandwidth enhancement significantly because the space of the inner HMSIW ground has full with the length U-slot. The U-slot position influences the reflection coefficient deeper as shown in Fig. 5(c). The U-slot position influences the TE_{101} from inner HMSIW to become shifting into the lower frequency.

D. Antenna Polarization

Antenna design has dual polarization i.e. linear and circular polarization along an impedance bandwidth range as shown in Fig. 6. It occurs because of the combination of two TE modes

from the inner and outer HMSIW cavities. The linear polarization occurs at 5.68 – 6.50 GHz and 6.55 – 6.59 GHz while the circular polarization occurs at 6.50 – 6.55 GHz with 0.77%. Circular polarization occurs because the amount of electric field generated in the phi and theta directions has the same magnitude. Also, the differentiation between phi and theta direction was 90°. This antenna design has many radiation vectors of the electric field which when decomposed to phi and theta fulfill the requirements of circular polarization.

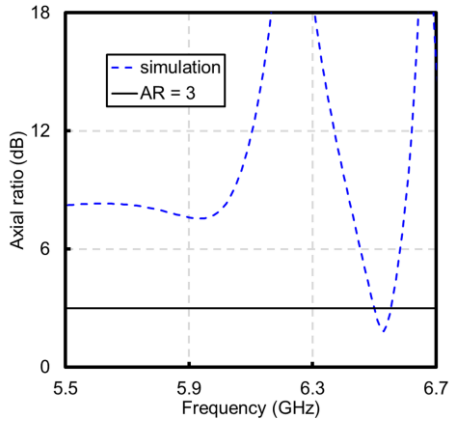

Fig. 6. The axial ratio bandwidth for antenna design (Ant-C)

E. Radiation Pattern and Gain Antenna

Antenna design has dual-direction radiation patterns as shown in Fig. 7 for hybrid resonance frequencies. The dual direction occurs because the rectangular slot on the patch and the U-slot on the ground have electric field vectors that radiate into the free air. It is proven by the electric field distribution as shown in Fig. 3.

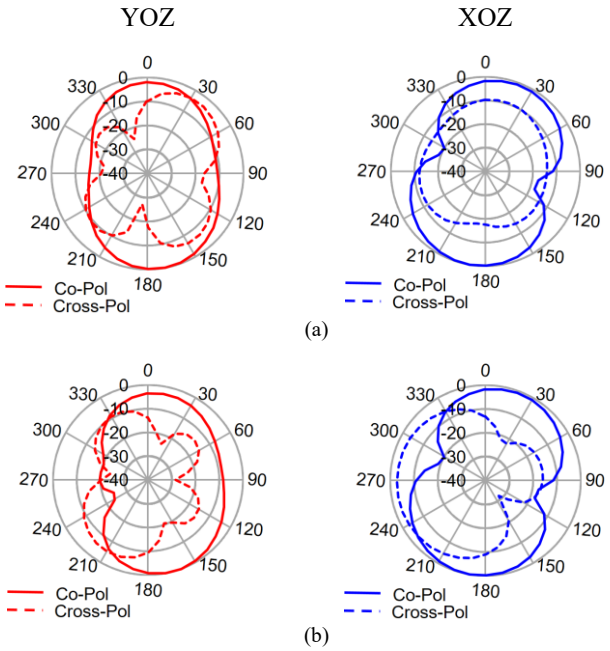

Fig. 7. The radiation pattern for antenna design on (a) 6 GHz, and (b) 6.48 GHz

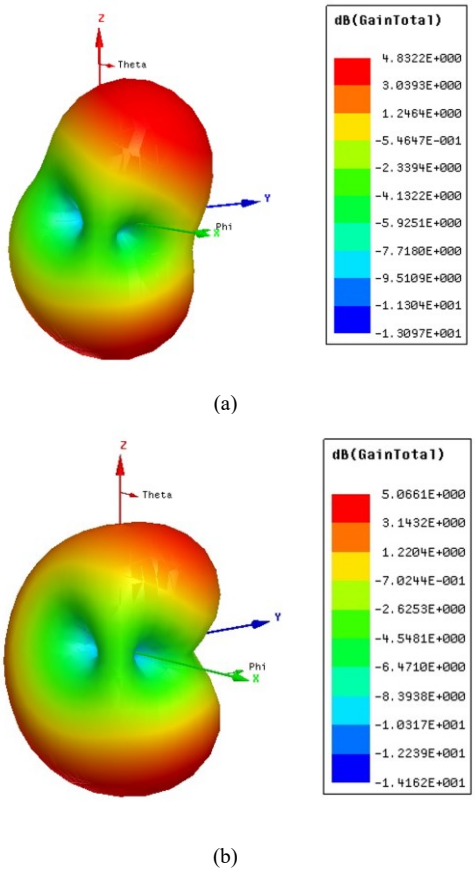

Fig. 8. The gain total for antenna design on (a) 6 GHz, and (b) 6.48 GHz

The gain total simulation for antenna design has 4.83 dBi on 6 GHz and 5.07 dBi on 6.48 GHz. The 3D polar plot for each frequency resonance is shown in Fig. 8(a) and (b). The dual radiation pattern is also seen on the 3D polar plot.

III. Result and Discussion

The antenna design is fabricated by photo etching process as shown in Fig. 9. The antenna is validated by using measurement. The reflection coefficient simulation and measurement are shown in Fig. 10. The reflection coefficient was measured at 14.31% (5.71 – 6.59 GHz) while the reflection coefficient simulated has 14.83% (5.68 – 6.59 GHz). The good agreement between simulation and measurement results for the reflection coefficient parameter.

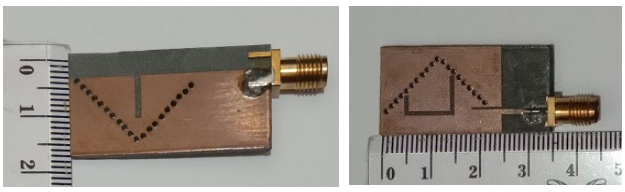

(a) (b)

Fig. 9. Fabrication antenna: (a) the patch view, (b) the ground view

TABLE I
THE COMPARISON BETWEEN THE PROPOSED ANTENNA DESIGN WITH THE PREVIOUS RESEARCH

Ref.	SIW CBS Antenna Method	Number resonance	Frequency (GHz)	Dimension (λ_0^3)	Substrate thickness (mm)	Fractional bandwidth (%)
[4]	Rectangular slot	hybrid	9.96	0.03 × 0.59 × 0.41	0.508	6.32
[5]	Bow-tie slot	hybrid	10.92	0.03 × 0.65 × 0.58	0.787	9.43
[6]	Unequal dual slot	triple	8.53	0.03 × 0.55 × 0.42	0.51	8.53
[10]	Rectangular slot	single	8.58	0.03 × 1.01 × 0.48	0.78	4.9
[11]	Rectangular slot	single	2.45	0.12 × 0.35 × 0.23	1.575	1.22
[12]	Semi-hexagonal slot	single	5.8	0.05 × 0.85 × 0.40	1.524	2.59
[13]	Fraction mode	quad	3.55	0.08 × 0.43 × 0.43	3	13.52
[14]	Square patch coupling	hybrid	7.94	0.04 × 0.81 × 0.61	0.787	11.21
[15]	Circular slot	hybrid	27.49	0.01 × 0.65 × 0.26	0.508	12.84
[17]	Triangular slot	hybrid	3.85	0.08 × 0.40 × 0.40	1.575	9.87
[18]	Epsilon slot	triple	5.45	0.06 × 1.04 × 0.58	1.575	13.29
This work	U-slot as a DGS	hybrid	6.15	0.05 × 0.72 × 0.37	1.575	14.31

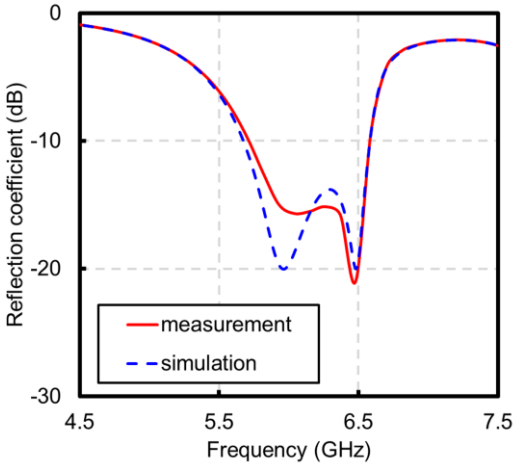

Fig. 10. Reflection coefficient simulation and measurement

Table I shows the comparison between the proposed antenna design with the previous research. The proposed antenna design with a U-slot as a DGS has a higher impedance bandwidth rather than other research reports. The proposed antenna design has an impedance bandwidth of up to 14.31% with hybrid resonant frequencies.

CONCLUSION

A substrate-integrated waveguide (SIW) cavity-backed slot antenna (CBSA) with defected ground structure (DGS) has been proposed in this paper. The rectangular slot and the U-slot as DGS has enhanced impedance bandwidth by resulting in hybrid resonant frequencies. The first resonant frequency has resulted from the combination of the TE_{101} modes from inner and outer HMSIW cavities while the second resonant frequency has resulted from the combination of the strong TE_{101} and the weak TE_{102} mode from the inner cavity and the addition of the weak TE_{101} from the outer cavity. The hybrid resonant frequencies were analyzed by the electric field distribution. The fabrication and measurement have shown that the antenna design with the DGS has enhanced impedance bandwidth up to 14.31% (5.71 – 6.59 GHz). It proves that the DGS can be implemented into SIW CBSA.

REFERENCES

[1] M. Bozzi, A. Georgiadis, and K. Wu, "Review of Substrate-Integrated Waveguide Circuits and Antennas," *IET Microwaves, Antennas Propag.*, vol. 5, no. 8, pp. 909–920, 2011. https://doi.org/10.1049/iet-map.2010.0463

[2] G. Q. Luo, Z. F. Hu, L. X. Dong, and L. L. Sun, "Planar Slot Antenna Backed by Substrate Integrated Waveguide Cavity," *IEEE Antennas Wirel. Propag. Lett.*, vol. 7, pp. 236–239, 2008.

[3] S. Yun, D. Y. Kim, and S. Nam, "Bandwidth and Efficiency Enhancement of Cavity-Backed Slot Antenna Using a Substrate Removal," *IEEE Antennas Wirel. Propag. Lett.*, vol. 11, pp. 1458–1461, 2012. https://doi.org/ 10.1109/LAWP.2012.2230392

[4] G. Q. Luo, Z. F. Hu, W. J. Li, X. H. Zhang, L. L. Sun, and J. F. Zheng, "Bandwidth-Enhanced Low-Profile Cavity-Backed Slot Antenna by Using Hybrid SIW Cavity Modes," *IEEE Trans. Antennas Propag.*, vol. 60, no. 4, pp. 1698–1704, 2012.

[5] S. Mukherjee, A. Biswas, and K. V Srivastava, "Broadband Substrate Integrated Waveguide Cavity-Backed Bow-Tie Slot Antenna," *IEEE Antennas Wirel. Propag. Lett.*, vol. 13, pp. 1152–1155, 2014. https://doi.org/ 10.1109/LAWP.2014.2330743

[6] M. Mbaye, J. Hautcoeur, L. Talbi, and K. Hettak, "Bandwidth Broadening of Dual-Slot Antenna Using Substrate Integrated Waveguide (SIW)," *IEEE Antennas Wirel. Propag. Lett.*, vol. 12, pp. 1169–1171, 2013. https://doi.org/ 10.1109/LAWP.2013.2281295

[7] A. Kumar, M. Kumar, and A. K. Singh, "Substrate Integrated Waveguide Cavity Backed Wideband Slot Antenna for 5G Applications," *Radioengineering*, vol. 30, no. 3, pp. 480–487, 2021.

[8] D. W. Astuti, R. Fadilah, Muslim, D. Rusdiyanto, S. Alam, and Y. Wahyu, "Bandwidth Enhancement of Bow-tie Microstrip Patch Antenna Using Defected Ground Structure for 5G," *J. Commun.*, vol. 17, no. 12, pp. 995–1002, 2022.

[9] M. K. Khandelwal, B. K. Kanaujia, and S. Kumar, "Defected Ground Structure: Fundamentals, Analysis, and Applications in Modern Wireless Trends," *Int. J. Antennas Propag.*, vol. 2017, pp. 1–22, 2017. https://doi.org/ 10.1155/2017/2018527

[10] D. W. Astuti, I. Wahyuni, and M. Alaydrus, "Lowpass Filter with Hilbert Curve Ring and Sierpinski Carpet DGS," *TELKOMNIKA*, vol. 16, no. 3, pp. 1092–1100, 2018.

[11] S. A. Razavi and M. H. Neshati, "Development of a Linearly Polarized Cavity-Backed Antenna Using HMSIW Technique," *IEEE Antennas Wirel. Propag. Lett.*, vol. 11, pp. 1307–1310, 2012. https://doi.org/10.1109/LAWP.2012.2227231

[12] D. W. Astuti and E. T. Rahardjo, "Size Reduction of Cavity Backed Slot Antenna using Half Mode Substrate Integrated Waveguide Structure," *4th Int. Conf. Nano Electron. Res. Educ. Towar. Adv. Imaging Sci. Creat. ICNERE 2018*, pp. 1–4, 2018. https://doi.org/10.1109/ICNERE.2018.8642564

[13] D. Chaturvedi and S. Raghavan, "A Half-Mode SIW Cavity-Backed Semi-Hexagonal Slot Antenna for WBAN Application," *IETE J. Res.*, pp. 1–7, Apr. 2018. https://doi.org/10.1080/03772063.2018.1452644

[14] B. J. Niu and J. H. Tan, "Bandwidth Enhancement of Low-Profile SIW Cavity Antenna using Fraction Modes," *Electron. Lett.*, vol. 55, no. 5, pp. 233–234, 2019. https://doi.org/10.2528/PIERL18102505

[15] H. Dashti and M. H. Neshati, "Development of low-profile patch and semi-circular SIW cavity hybrid antennas," *IEEE Trans. Antennas Propag.*, vol. 62, no. 9, pp. 4481–4488, 2014. https://doi.org/10.1109/TAP.2014.2334708

[16] Q. Wu, H. Wang, C. Yu, and W. Hong, "Low-Profile Circularly Polarized Cavity-Backed Antennas Using SIW Techniques," *IEEE Trans. Antennas Propag.*, vol. 64, no. 7, pp. 2832–2839, 2016. https://doi.org/10.1109/TAP.2016.2560940

[17] D. W. Astuti, Y. Wahyu, F. Y. Zulkifli, and E. T. Rahardjo, "Hybrid HMSIW Cavity Antenna with a Half Pentagon Ring Slot for Bandwidth Enhancement," *IEEE Access*, vol. 11, no. February, pp. 18417–18426, 2023. https://doi.org/10.1109/ACCESS.2023.3247604

[18] D. W. Astuti, M. Asvial, F. Y. Zulkifli, and E. T. Rahardjo, "Bandwidth Enhancement on Half-Mode Substrate Integrated Waveguide Antenna Using Cavity-Backed Triangular Slot," *Int. J. Antennas Propag.*, vol. 2020, 2020. https://doi.org/10.1155/2020/1212894

[19] D. Chaturvedi, A. Kumar, and S. Raghavan, "Wideband HMSIW-Based Slotted Antenna for Wireless Fidelity Application," *IET Microwaves, Antennas Propag.*, vol. 13, no. 2, pp. 258–262, 2019. https://doi.org/10.1049/iet-map.2018.5110

[20] F. Xu and K. Wu, "Guided-Wave and Leakage Characteristics of Substrate Integrated Waveguide," *IEEE Trans. Microw. Theory Tech.*, vol. 55, no. 1, pp. 66–73, 2005.
https://doi.org/10.1109/TMTT.2004.839303

[21] D. Pozar, *Microwave Engineering Fourth Edition*. 2005.